IOWA STATE UNIVERSITY
Digital Repository

10-2013

A feasibility study of wind turbine blade surface crack detection using an optical inspection method

Huiying Yu
Iowa State University, yuhuiying89@gmail.com

John K. Jackman
Iowa State University, jkj@iastate.edu

Follow this and additional works at: http://lib.dr.iastate.edu/imse_conf

A feasibility study of wind turbine blade surface crack detection using an optical inspection method

Huiyi Zhang[1], John Jackman
Wind Energy Manufacturing Laboratory
Dept. of Industrial and Manufacturing Systems Engineering, Iowa State University Ames, IA 50011 U.S

Abstract — **A new image processing technique was investigated to assess its ability to detect surface flaws on an on-tower wind turbine blade (WTB). The method was tested by varying the parameters of the surface flaws as well as the parameters of the method. It was found that detecting and quantifying cracks as small as hair thickness with computer-based optical inspection is feasible and the orientation of a crack was not sensitive to image processing so that the inspection camera does not need to be set up at a specific angle to detect cracks. It was also found that uneven background illumination was significantly reduced by optimizing the threshold value using the *Canny* method. In addition, the accuracy of quantifying a crack was improved by reducing noise with the intersection of two processed images from *Sobel* and *Canny* methods.**

Keywords—gel coat cracks, optical inspection, blades, O&M

I. INTRODUCTION

Wind energy provides more than 3% of total U.S. electricity supply and contributes more than 10% of total electricity generation in six states with two of these states being above 20% [1]. Most of the wind farms have installed turbines in the past 10 years and the installation capacity is expected to grow continuously at more than 25% per year to reach the 20% level of total electric generating capacity in the scenario proposed by the Department of Energy (DOE) by 2030 [2]. Although the design life of a wind turbine is often claimed to be 20 years, early failure can affect critical components and cause significant down time, causing concern for power generation companies and investors. Rotor blades are one of the largest mechanical components of a wind turbine and cannot be monitored as easily as electrical parts/controllers and smaller mechanical components such as bearings inside the nacelle. The limited monitoring ability of current Operation and Maintenance (O&M) functions for wind farms can lead to higher energy costs. In addition, the general public has voiced a number of concerns about the viability of wind energy. To address part of the viability and cost concerns, research on reliable and cost-effective blade monitoring systems is warranted.

Rotor blades account for roughly 18% of the total turbine cost and maintenance poses significant challenges due to the scale, on-tower location, and the use of multiple materials in blades. The annual O&M cost of a wind farm is estimated to be 0.5 – 2.5 /kWh based on the generating capacity and number of operating years, accounting for 10 - 20% of the total cost of energy (COE) for a wind project, based on current COE figures of 3.5 – 6 cents/kWh [3]. Although there is little information on cost breakdown of components for O&M, blade failure ranks in the top third of failure rates among all the critical large mechanical components. In addition, blade failure causes significant downtime (four days on average) and repair requires expensive equipment (e.g., cranes) and skilled technicians [4]. Early inspection can help prevent severe structural damage and reduce O & M costs [5]. A report by the SGS Group points out that a major blade incident costs 26% of the total turbine blade sales price to repair. Repairing before the major incident with the help of a third-party inspection company though would cost only 0.64% of the turbine blade sales price.

In recent years, developing a cost-effective blade inspection system has received more attention both in academia and industry. Since blades are large-scale and on-tower, image acquisition has been the focus of many efforts, but analysis of images has not received much attention. This paper investigated techniques to identify and quantify general blade surface defects consistently and accurately.

II. RELATED WORKS

A. Development of visual inspection

Optical inspection is widely used to improve the reliability of in-service large scale products such as WTBs, aircraft surfaces, and bridges. Motivating factors for adopting reliable optical inspection techniques include (1) lowering costs by reducing maintenance hours, (2) increasing labor safety, and (3) decreasing production and service downtimes. Current WTB inspection is typically performed by "sky workers" (i.e., technicians) tethered to the nacelle while they perform close-up inspection and repair or at a distance using telescopes, which can be used to capture blade surface images from the ground. It is widely known that manual inspection techniques in general are inconsistent because inspectors use their judgment as to what constitutes a flaw and may overlook a flaw.

In composite manufacturing, visual inspection was adopted early to inspect commercial aircraft surfaces for defects. An aircraft surface inspection is typically composed of 90% visual inspection and 10% Non-destructive Inspection (NDI) [6]. NDI is a well-accepted method for finding internal defects in composites. Image-based surface inspection can be used to determine whether NDI is necessary or not. Currently, inspection methods depend heavily on human eyes. This method is time consuming and has poor accuracy. Remote visual inspection tries to address these issues.

Mumtaz described a mobile inspection unit called the Crown Inspection Mobile Platform [7]. This unit combines

contourlet transform and discrete cosine transformation to find the edges of flaws on an aircraft surface. Countourlet transform can efficiently identify the intrinsic geometrical structure containing contours by filtering discontinuous points. Discrete cosine transformation was used to extract features and to recognize patterns. However, it has only been tried on a small sample set of simulated cracks. The authors stated that the system must be applied to many new types of cracks and surface issues before it can begin to replace human visual inspections. The extent of crack detail that can be recognized and how to handle the missing data due to the uneven illumination of the image background were not addressed

Some researchers are now trying to develop automatic visual inspection systems for WTBs to make use of the robot inspection methods. WTB surface images tend to have more noise compared to aircraft since blade surfaces are not cleaned frequently like aircraft surfaces. Also, blade surface images have more uneven illumination due to the large scale, complex geometry, and uncontrolled lighting.

A new approach is to use a climbing robot with a ground-based control station to scan rotor blades with a high resolution camera (see Fig. 1) [8]. Image processing techniques or experienced engineers then analyze the robots' images. Rosa developed a low-cost climbing robot for offshore wind turbine blades inspection in 2002 [9]. General Electric (GE) and International Climbing Machines (ICM) have developed a remote controlled wall climbing robot with a wireless high resolution video camera attached to its back to capture blade surface images. Fraunhofer Institute for Factory Operation and Automation IFF developed a robot called RIWEA that can register the exact positions of cracks and delaminations [10]. Both of these robots require post-image processing. The literature has not addressed the degree to which a crack can be recognized by image processing. Both of these methods are still under development or testing and the cost has not been addressed at this time. Another disadvantage is that these robots cannot capture images while the WTBs are rotating.
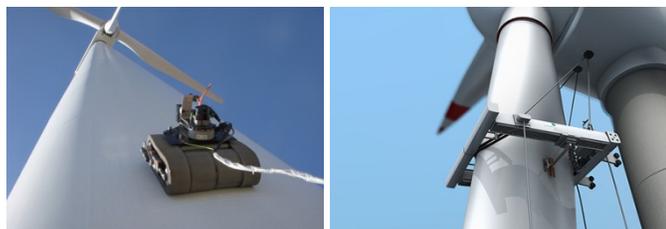

Fig. 1. Climbing robot [8] and RIWEA [10]

B. Review of blade surface defects

Many turbine blades are coated with two thin layers, a gel coat layer and an environmentally friendly water-based varnish, to prevent infiltration of moisture, sand, and salt into the underlying fiberglass composite material which can lead to delamination and other types of structural damage. "Depending on the stress applied to the blade surface, the thickness of the gel coat may vary between 0.3mm where loads are light and 0.6mm along the leading edge where it makes first contact with wind and loads are particularly high [11]." The health of a blade skin is a major maintenance concern and is a significant contribution to energy cost using existing on-tower inspection and repair methods. With wind energy moving offshore, the rotor blades will experience a more challenging environment – high moisture and salt – and higher maintenance costs.

Typically, in-service WTBs have surface defects in the following categories.

- Erosion, also called pitting and wear, is most likely along the leading edge and blade tips.
- Cracks in a gel coat or paint layer, channel cracks, stress cracks
- Skin debonding contains paint peeling, gel coat cracking, and gel coat/skin debonding

Cracks become visually apparent as discontinuities in a surface consisting of multiple segments, where the surface has split without breaking into separate parts. Various industries have tried to observe and characterize surface cracks. "Cracks usually have low luminance and can be considered as local intensity minima with rather elongated structural characteristics" [12]. It is critical to determine whether the crack is in the surface coating, like a scratch, or whether the crack affects inner laminations. However, this determination can only be inferred from 2-D images.

Many early defects are hairline thickness cracks along the gel coat layer. Gel coat cracks have various forms that can be found at the root section of the rotor blades, or along the leading edge and surfaces along the spar cab. Gel coat cracks can have a single cause and multiple causes.

Typical gel coat cracks are stress cracks, crazing, and thermal cracks. All of them can significantly reduce the aerodynamic efficiency of blades and lead to structural damage, which is more challenging to detect and repair. This paper addresses the characteristics of a WTB surface crack and method parameters for computer-aided optical inspection. Similar methods have been considered in aircraft health inspection. For example, a stereoscopic method has been successfully applied for a limited number of surface cracks on aircraft skins [16]. Therefore, further investigation is warranted to assess the capability of image processing techniques in the detection of cracks in the gel coat layer.

III. METHODOLOGY

A series of synthetic cracks were generated to understand the common characteristics of a surface crack and the factors that define its visibility. The reason why synthetic cracks were used is because the available crack image pool is limited and it was necessary to control the fundamental characteristics of a crack. Brownian motion was used to create a random crack with correlation between neighboring points on the crack. Variations in thickness and color were also included. Line and edge segmentation algorithms were developed to detect hairline and nontrivial thickness cracks. Line detection was applied first to provide the capability of a quick overall scan of images of blade surfaces and then the edge detection method was used to extract smoothing information from the original images. The goal was to assess how much detail of a surface defect could be found with digital image processing. In addition to understanding the detectability of the method, it

was necessary to consider potential errors that image processing might introduce. A defect quantification algorithm was developed to quantify the recognized surface defects. Finally, the method was tested on a group of well-selected site images and the findings are addressed in the results section.

A. Sample cracks generation

To understand detectability, a set of representative synthetic cracks was generated with one dimensional (1D) Brownian motion to create samples in a controlled fashion as shown in Fig. 2. "1D Brownian motion is composed of a sequence of normally distributed random displacements and their sum represents a particle trajectory in one dimension" [13]. The reason to use 1D Brownian, rather than 2D is that 2D Brownian has random moving particles along both x and y axes and their sums do not form a crack-like geometry. In addition, the intensity level of pixels of the synthetic crack itself was varied to represent the severity of a crack. The background color of the synthetic cracks was defined as either white or light gray to be consistent with the paint color of a rotor blade. The color of surface cracks gradually changes as the cracks go deeper into the surface and become easier to identify in digital images. The complexity of a synthetic crack was reflected in its non-uniform thickness, variation in color, and small derivative cracks.
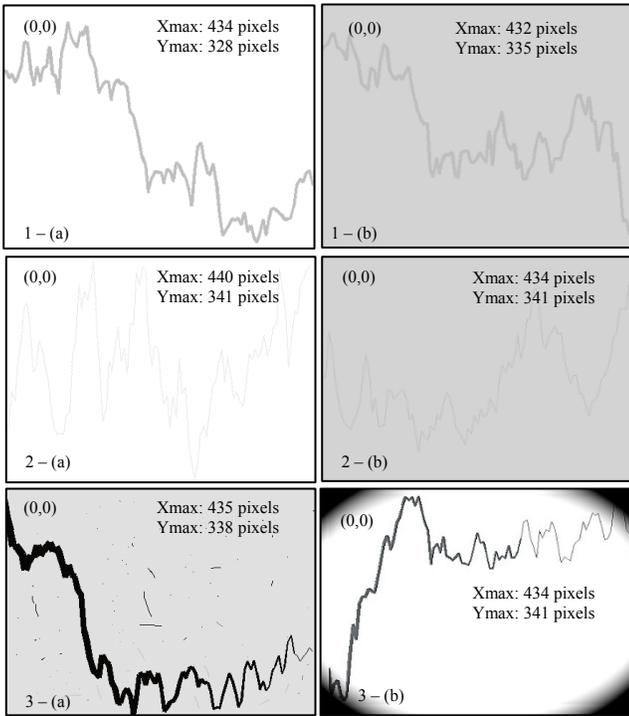

Fig. 2. Syntheic cracks: Group 1, 2, and 3.

Difference in the intensity level of pixels, irregular distribution and geometry of noise, and uneven illumination of the image background are three major concerns that can significantly decrease the detectability of a crack [14]. Also the geometry and color of a crack may have some level of impact on the defect detectability. Therefore, we generated three representative groups of synthetic cracks as shown in Fig. 2. Synthetic cracks can better represent the random nature of

cracks because they are more flexible for manipulating the key parameters of a crack. The only difference between the synthetic cracks in group 1 is the intensity level of the pixels on the background. The second group was used to examine if computer-based optical inspection can find defects that are difficult to see with the human eye. The third group included the effect of severe noise and uneven illumination.

Three field images were selected to further evaluate whether the parameters that define detectability are consistent with the six synthetic cracks, see Fig. 3. After testing the method on the three groups of synthetic cracks, the field images were used to evaluate the accuracy of the method. The first field image was a hairline crack and was recognized as the most difficult flaw to detect with the human eye. The hairline cracks shared the same characteristics as the synthetic cracks in the second group. The second image was a stress crack. It was used to understand the impact of uneven illumination to the detectability of an image. A third crack was crazing, which typically has a spiderweb geometry and some of the small cracks in a crazing may not follow along the four directions of standard line detectors. In addition, the third crack has severe background noise.
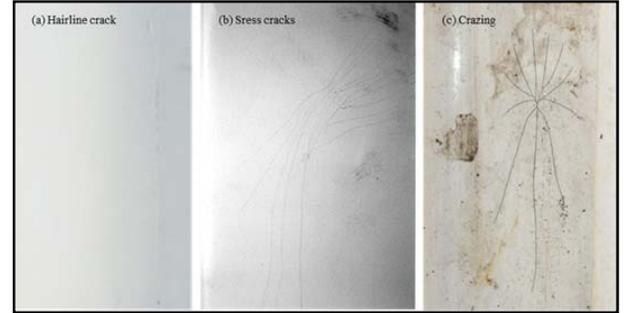

Fig. 3. Representative field images: (a) Hairline crack, (b) Stress crack, and (c) Crazing.

B. Line detection

A line detection method was used to perform a quick scan that could be used on a large scale WTB. It is simple, fast, and sensitive to individual line segments. Cracks can be treated as a set of segments. A line is a basic type of intensity discontinuity in a digital image and the most common method to detect them is to process the image with a linear spatial filter mask with a binary format. The process consists of moving the center of the mask from point to point in an image and computing the response at each point, which is the sum of the product of the mask coefficients and the corresponding neighborhood pixels lies in the area spanned by the mask and is given by

$$R = \sum_{i=1}^{n} w_i z_i \qquad (1)$$

where, z_i is the intensity of the pixel associated with the mask coefficient w_i.

The smallest mask is a 3×3 matrix and there are four standard line detection masks corresponding to the orientation of the lines, namely, horizontal, 45°, vertical, and -45°. The larger number – 2 – in the mask matrix represents the direction of the mask and it has a strong response to one pixel thickness

segments. Increasing the number from 2 to 3 smoothed the output image but continually increasing the number will create fuzzy results. Although the vertical line detector masks responded strongly to one pixel thickness lines, it can recognize all vertical lines with different thicknesses. A binary union operation combines the detection results of the four standard line detector masks and offers more complete results.

TABLE I.   STANDARD LINE DETECTOR MASKS (A) HORIZONTAL. (B) 45˚. (C) VERTICAL. (D) -45˚

-1	-1	-1		2	-1	-1		-1	2	-1		-1	-1	2
2	2	2		-1	2	-1		-1	2	-1		-1	2	-1
-1	-1	-1		-1	-1	2		-1	2	-1		2	-1	-1

What if there was part of a crack in the image that was not oriented the same as the four masks above? Then it is difficult to use line detector masks for every possible direction of lines. However, one method is to rotate the image counterclockwise with a user defined step size while keeping the masks stationary, say 10˚. After line detection, we can rotate the image back to its original orientation and take the union operation, which maps the detected flaws from each rotation step to one united matrix. Therefore, the line detection method will be able to detect more defects that were limited by the direction of the line detector mask. However, it can slow down the detection speed if the mask rotational angle is small, say 1˚.

C. Edge detection

One major advantage of edge detection is that uneven illumination will not decrease the detectability. Edge detection was used to capture the outer contour of non-uniform thickness cracks and to complement the inadequacy of line detectors for detecting meaningful discontinuities in intensity values. Unlike line detection, edge detection uses first- or second-order derivatives to compute the maximum rate of change of gray levels of pixels. Edge detection gave much smoother results while eliminating noise that will probably miss one pixel thickness hairline cracks. Therefore, line detection was applied first so that a quick overall scan of images of rotor blade surfaces could be performed in a reasonable amount of time. Afterwards, the edge detection method was used to extract smoothing information from the areas identified by the line detection.

MATLAB has a function, *edge*(), that supports several common detectors: *Sobel, Prewitt, Laplacian of a Gaussian (LoG),* and *Canny*. The key difference between these methods can be found in how the first or second-order derivatives are approximated. The first-order derivative in image processing is called gradient and is a vector for a 2D function $f(x, y)$ given by

$$\nabla f = \begin{bmatrix} G_x \\ G_y \end{bmatrix} = \begin{bmatrix} \frac{\partial f}{\partial x} \\ \frac{\partial f}{\partial y} \end{bmatrix} \tag{2}$$

with the magnitude of the vector as $g = mag(\nabla f) = [G_x^2 + G_y^2]^{1/2}$ and angle as $\alpha(x, y) = \tan^{-1}(\frac{G_x}{G_y})$,where the angle defines the edge direction. Both *Sobel* and *Canny* methods were considered since *Sobel* is most the commonly used and *Canny* is considered to be the most powerful edge detector. The *Canny* method is more complex and includes a Gaussian filter, a local gradient and edge direction computation algorithm, and provides edge linking [14].

D. Optimizing threshold

A threshold number is used to convert a gray-scale image to a binary image. Suppose $f(x, y)$ is an image and T is a selected threshold number, any point $(x, y) \geq T$ turned to 1 and is called an object point. Otherwise, the point turned to 0 and is called background point. A threshold image $g(x, y)$ is defined as

$$g(x, y) = \begin{cases} 1 \ if \ f(x, y) \geq T \\ 0 \ if \ f(x, y) < T \end{cases} \tag{3}$$

The default threshold number generated by *Sobel* or *Canny* does not guarantee a positive result. Both of *Sobel* and *Canny* offer promising results by optimizing the threshold value, but require a lot of human intervention, which is not desirable. In our method, the default threshold number was used first and then the threshold number was updated gradually. The edge detection method was applied again and the results were compared with the previous results to see if the difference was within an acceptable tolerance. The tolerance can be defined as the standard deviation of all results that lie in $(A_0 \cap B_0, A_0 \cup B_0)$, where A_0 is the result of *Canny* method with its default threshold and B_0 is the result of *Sobel* method with its default threshold. For instance, the default threshold value of *Canny* method is $T = [t_1, t_2]$ and the result is a matrix A_1 that contains all the detected edges along the cracks. The threshold value was updated using $T_2 = [t_1 + .1 \times (t_2 - t_1), t_2 + .1 \times (t_2 - t_1)]$ and the *Canny* algorithm was applied again with results A_2. Repeat the routine until $A_{i+1} - A_i \leq D$, where D is the tolerance. Both *Sobel* and *Canny* methods produce recognizable edges. The major differences between *Sobel* and *Canny* were the amount and geometry of noise.

E. Quantifying the size of a crack

Two methods were used to quantify the magnitude of a crack. The first and also the easiest method was to find the minimum enclosing rectangle (parallel to the x and y axes) that enclosed the points along the crack. This defined the most likely required repair area. However, it did not give any further information about the orientation of the crack and tended to overestimate the magnitude.

The second approach was to define the minimum enclosing rectangle that was not oriented with respect to the x and y axes. This could be found by estimating the parameters of a line that minimizes the maximum distance to all the points on the crack edges. Using the start and end points of the line by finding the end points on the edges along the line, the sides of the rectangle are found by projecting the end points onto the estimated line. The other two sides are determined by the maximum deviation of the crack on each side of the line. In order to minimize the maximum distance to the line, the function *fminimax* in MATLAB was selected to find the best fit parametric line, denoted by

$$\begin{cases} x = at + b \\ y = ct + d \end{cases} \tag{4}$$

The function, *fminimax*, requires an initial guess for the parameters of the line [a, b, c, d] and a function that computes the maximum distance of all points along the edges to the given line. The function stops when the values of [a, b, c, d] are within a specified tolerance or reach the maximum number of iterations. The default iteration limit is 500 in MATLAB. In this study a limit of 2500 iterations was used. Since it is difficult to display t on the graph, the line function was converted to slop-intercept form, $y = mx + b$ in the results section.

F. Two kinds of errors

Computer-based crack detection methods (as well as manual inspection) can result in two kinds of errors: false-positive identification of cracks (Type 1) and failure to detect existing cracks (Type 2). Type 1 errors can be caused by noise, which cannot be totally avoided. If the noise is significant, then it is difficult to quantify the crack accurately. Type 2 errors may occur due to non-uniform illumination of the image background. The consequences of a Type 1 error in this context are not as severe as the Type 2 error, since missing defects can lead to ignoring the necessary maintenance, leading to future structural damage. Type 2 error can be reduced significantly by optimizing the threshold number.

IV. RESULTS

The six synthetic cracks and three representative field images were tested with both line and edge detection methods. Although there is a tradeoff between Type 1 Error and Type 2 Error, *Canny* produced the best results by far in terms of reducing the two types of error. Generally, the line detection method was very sensitive to discontinuity and thus, the detected results had more Type 1 errors as compared to edge detection methods. However, this is not in conflict with our goals that line detection could be used as a quick scan of the entire turbine. In addition, the orientation of a crack did not affect the detectability of the line detection method as shown in Fig. 4.
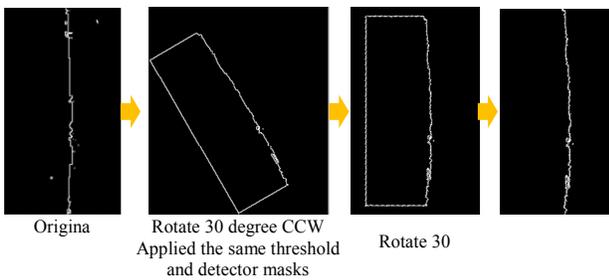

Fig. 4. Hairline crack with different orientations

Uneven illumination is not a major factor in edge detection methods and noise can be significantly reduced with the optimized threshold algorithm as shown in Fig. 5. Therefore, the edge detection algorithm minimizes Type 1 error, which includes the optimized threshold algorithm (see Fig. 6, 7).

The units of the boundary boxes in Fig. 6 and 7 are in pixels which can be converted to mm if there is dimensional information associated with the image. The location of the cracks can be inferred with the whole blade images.
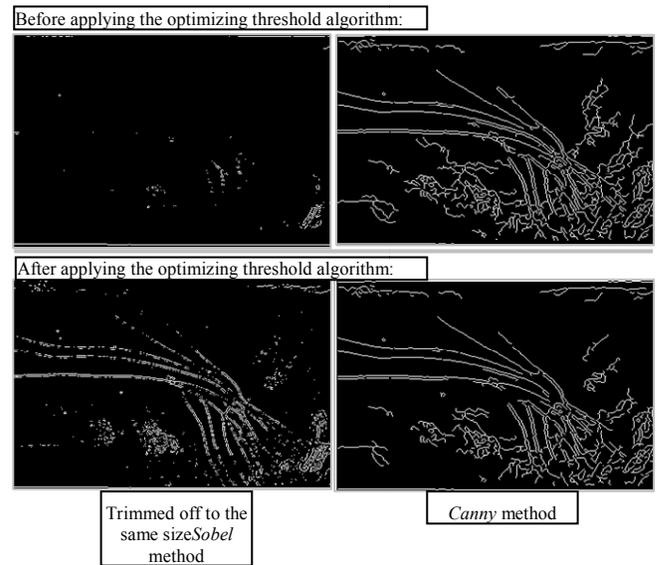

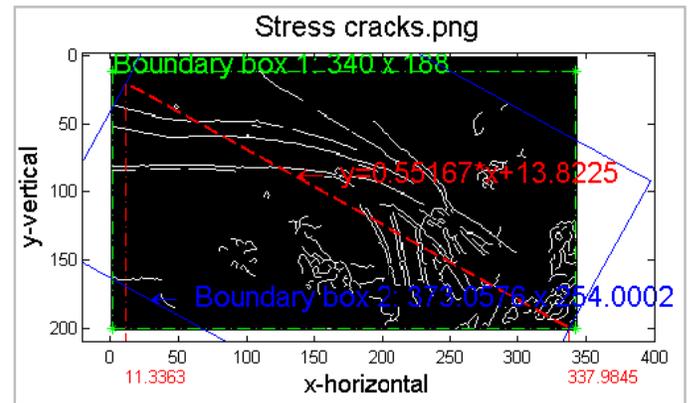Fig. 5. Optimizing threshold with Fig. 2-(b) Stress crack

Fig. 6. Quantification of the field image in Fig. 3 (b): rotated 90 degree C.W. Approximation line function: $y = 0.55x + 13.82$. Boundary box 1: 340 x 188 pixels. Bounday box 2: 373 x 254 pixels
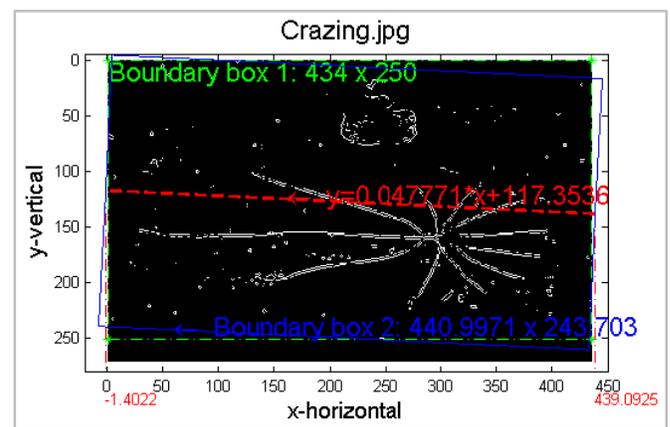

Fig. 7. Quantification of the field image in Fig. 3 (c): rotated 90 degree C.W. Approximation line function: $y = 0.05x + 117.35$. Boundary box 1: 434 x 250 pixels. Bounday box 2: 440 x 244 pixels

The severity of a crack is difficult to quantify. However, the quantifying crack algorithm offers important information about a crack such as size and direction. Also, the depth of a

crack can be inferred from the intensity levels of the pixels along the detected edges. If an image contains severe Type 1 error, the parallel lines drawn by the defect quantification algorithm will also contain the noise as shown in Fig. 6, 7. This indirectly explained why it was important to minimize background noise.

Environmental noise like dirt or insects caused problems with the accuracy of quantifying surface flaws as shown in Fig. 7, because it could not be identified and eliminated in 2-D images. Also, noise had more of an impact in images with uneven illumination, making it more difficult to eliminate noise. Further study on identifying and minimizing noises is important for the computer-based optical inspection method.

V. CONCLUSION AND FUTURE WORK

This paper evaluated two computer-based methods for detecting cracks in wind turbine blades: the line detection method and the edge method. We initially thought that the line detection method would be best for performing a quick scan of the blade surface to find cracks, and that the edge method would provide better data on the crack. The results of this study supports our hypothesis.

The line detection method is appropriate for quick scans because it can quickly identify hairline cracks that may be missed by the human eye. Image processing thresholds and filters can be used to minimize false-positives caused by surface irregularities like dirt or dust. Uuneven illumination does not pose serious problems to the edge detection. The edge detection method also gave much smoother results. The most effective method we identified was to first identify the cracks using line detection and only then apply edge detection to collect more information on the crack. Edge detection is particularly useful when there is uneven illumination.

The crack quantifying algorithm produces important information for site engineers. However, environmental noise reduced the accuracy and could not be eliminated easily.

The results showed that the computer-based crack detection shows promise for maintenance work on in-service WTBs. With a high quality image and analysis tools, it is likely that greater consistency in crack detection can be achieved. Further research is necessary to apply these methods to more sample cracks and to refine the methods to minimize errors.

REFERENCES

[1] Chen, A., New Study Finds the U.S. Wind Power Market Riding a Wave That Is Likely to Crest in 2012. News Center, Lawrence Berkeley National Laboratory, August 14, 2012.

[2] National Renewable Energy Laboratory (NREL) Report, "20% Wind Energy by 2030: Increasing Wind Energy's Contribution to U.S. Electricity Supply." DOE/GO-102008, July 2008

[3] Walford, Christopher A., "Wind turbine reliability: Understanding and minimizing wind turbine operation and maintenance costs." Global Energy Concepts, LLC. Sandia Report: SAND2006-1100 Mar. 2006

[4] Hahn, B., Durstewitz, M., and Rohrig, K., "Reliability of Wind Turbine – Experiences of 15 years with 1,500 WTs." Institut für Solare Energieversorgungstechnik (ISET), Verein an der Universität Kassel e.V., 34119 Kassel, Germany.

[5] SGS Group, The cost of wind blade inspections versus blade repair. Hamburg, Germany, Retrieved from http://www.nacleanenergy.com/oldsite/index.php?option=com_content&view=article&id=2328%3Athe-cost-of-wind-blade-inspections-versus-blade-repair&Itemid=150

[6] Siegel, M., "Enhanced remote visual inspection of aircraft skin." Robot Institute. Carnegie Mellon University. Proceedings of the Intelligent NDE Sciences for Aging and Futuristic Aircraft Workshop, September, 1997, pp. 101 - 112.

[7] Mumtaz, M., "A new approach to aircraft surface inspection based on directional energies of texture." Pattern Recognition, Aug. 2010, pp. 4404-4407

[8] GE Reports, Go Go Gadget: Robotic crawler rides up 300-foot poles to inspect wind turbine blades. Jun. 13th, 2012 Retrieved from http://www.gereports.com/go-go-gadget/

[9] Rosa, Guido L., "A low-cost lightweight climbing robot for the inspection of vertical surfaces." *Mechatronics*, Volume 12, Issue 1, Feb. 2002, Pages 71-96

[10] Elkmann, N., *Robot for the inspection of wind turbine rotor blades (RIWEA).* Fraunhofer Institute for Factory Operation and Automation. Retrieved from http://www.iff.fraunhofer.de/en/business-units/robotic-systems/riwea.html

[11] ABB robotics, "ABB Robotics - Painting wind turbine rotor blades." Dec., 2009 Retrieved from http://robotize.com.au/robotic-news/videos/25ba98/ABB-Robotics---Painting-wind-turbine-rotor-blades/

[12] Giakoumis, L., "Digital Image Processing Techniques for the Detection and Removal of Cracks in Digitized Paintings." *IEEE Transaction on Image Processing*, Vol. 15, No. 1, January 2006

[13] EPFL, Dept. of Life Science and Technology Section, École Polytechnique Fédérale de Lausanne, Simulating Brownian motion. Retrieved from http://ssv.epfl.ch/files/content/sites/lben/files/users/179705/Simulating%20Brownian%20Motion.pdf

[14] Gonzalez, Rafael C., *Digital Image Using MATLAB Processing.* Upper Saddle River, New Jersey, Pearson Education, Inc., 2004.

[15] Marsh, G., "Meeting the challenge of wind turbine blade repair." *Reinforced Plastics,* July-August, 2011, Vol.55(4), p.32(5)